



# Characterization of the biosolids composting process by hyperspectral analysis



Talli Ilani<sup>a,1</sup>, Ittai Herrmann<sup>b,1</sup>, Arnon Karnieli<sup>b</sup>, Gilboa Arye<sup>a,\*</sup>

<sup>a</sup>French Associates Institute for Agriculture & Biotechnology of Drylands, The Jacob Blaustein Institutes for Desert Research (BIDR), Ben-Gurion University of the Negev, Israel

<sup>b</sup>The Remote Sensing Laboratory, Blaustein Institutes for Desert Research, Ben-Gurion University of the Negev, Sede Boker Campus, 84990, Israel

## ARTICLE INFO

### Article history:

Received 18 August 2015

Revised 25 November 2015

Accepted 26 November 2015

Available online 8 December 2015

### Keywords:

Compost

Biosolids

Hyperspectral spectroscopy

PLSR

## ABSTRACT

Composted biosolids are widely used as a soil supplement to improve soil quality. However, the application of immature or unstable compost can cause the opposite effect. To date, compost maturation determination is time consuming and cannot be done at the composting site. Hyperspectral spectroscopy was suggested as a simple tool for assessing compost maturity and quality. Nevertheless, there is still a gap in knowledge regarding several compost maturation characteristics, such as dissolved organic carbon, NO<sub>3</sub>, and NH<sub>4</sub> contents. In addition, this approach has not yet been tested on a sample at its natural water content. Therefore, in the current study, hyperspectral analysis was employed in order to characterize the biosolids composting process as a function of composting time. This goal was achieved by correlating the reflectance spectra in the range of 400–2400 nm, using the partial least squares-regression (PLS-R) model, with the chemical properties of wet and oven-dried biosolid samples. The results showed that the proposed method can be used as a reliable means to evaluate compost maturity and stability. Specifically, the PLS-R model was found to be an adequate tool to evaluate the biosolids' total carbon and dissolved organic carbon, total nitrogen and dissolved nitrogen, and nitrate content, as well as the absorbance ratio of 254/365 nm (E2/E3) and C/N ratios in the dry and wet samples. It failed, however, to predict the ammonium content in the dry samples since the ammonium evaporated during the drying process. It was found that in contrast to what is commonly assumed, the spectral analysis of the wet samples can also be successfully used to build a model for predicting the biosolids' compost maturity.

© 2015 Elsevier Ltd. All rights reserved.

## 1. Introduction

Biosolids are the by-products of wastewater treatment plants, commonly defined as a wastewater solid phase (the sewage sludge) that can be recycled as a soil amendment. The term biosolids, however, relates only to sewage sludge that undergoes a stabilization process, such as composting, before its application as a soil amendment. Applying composted biosolids to agricultural soils can be a suitable and sustainable solution for biosolid disposal, providing the crops with nutrients (Singh and Agrawal, 2008).

*Abbreviations:* DOC, dissolved organic carbon; OM, organic matter; TN, total nitrogen; PLS-R, partial least squares-regression; RMSEP, root mean square error of prediction.

\* Corresponding author at: French Associates Institute for Agriculture & Biotechnology of Drylands, The Jacob Blaustein Institutes for Desert Research (BIDR), Ben-Gurion University of the Negev, Sede Boqer Campus, Midreshet Ben Gurion, 84990, Israel. Tel.: +972 (0)8 6596747 (office), cell: +972 (0)52 4753844.

E-mail address: [aryeg@bgu.ac.il](mailto:aryeg@bgu.ac.il) (G. Arye).

<sup>1</sup> These authors contributed equally to this work.

Biosolid properties can vary greatly, depending upon their source materials and how they are processed. The source materials of the compost will affect the composting process, the properties and the quality of the final product. For instance, compost made from food residues is typically rich in nutrients and may have a high salt content (Hargreaves et al., 2008; Shah et al., 2014a). Yard waste compost is typically low in nutrients, contaminants and soluble salts (Shah et al., 2014a). Composted manure is generally high in nutrients and soluble salts, while low in contaminants (Moral et al., 2009). The composted sewage sludge is typically high in ammonium and soluble salt content (Smith et al., 1998). The concentration of pollutants such as heavy metals will vary greatly, depending upon which industrial waste products are discharged into the wastewater treatment plant.

It is well established that the application of composted biosolids to soil can contribute to its physical and chemical properties, thus improving the water and nutrient availability for plants (e.g., Ozores-Hampton and Peach, 2002; Rigby et al., 2009). On the other hand, the employment of immature composts may lead to the

immobilization of nutrients by microorganisms and can further cause phytotoxicity (Cambardella et al., 2003).

Stable compost is defined as organic matter (OM) that is resistant to further rapid degradation, and it can be measured by the respiration rate (Som et al., 2009). Mature compost is defined as compost suitable for plant growth, and it may be assessed by several variables such as seed germination, humification index, carbon (C) to nitrogen (N) ratio, cation exchange capacity, and OM loss (Wu et al., 2000). In order to measure these variables, compost samples should be taken to a lab for chemical analysis in each step of the composting process. The employment of these methods is time consuming, and commonly, more than one approach needs to be examined to reach a reliable deduction regarding the compost maturity.

To the best of our knowledge, a non-destructive and rapid method that can be employed in the composting plant in order to evaluate the stages of compost maturation and stability has not been established. Therefore, there is a need for a single simple method that can be applied on-site to evaluate compost's suitability for agricultural use.

Hyperspectral analysis has been widely used for mapping OM and nutrient content in soils (Bartholomeus et al., 2008; e.g. Boggs et al., 2003; Li et al., 2012; Liu et al., 2009; McMorrow et al., 2004; O'Rourke and Holden, 2012). In most studies, changes in OM properties were examined as a function of soil properties, such as OM, silt and clay content, and labile C and N (Anne et al., 2014). The above studies examined OM characteristics from one sampling event; only a handful number of studies have addressed the decaying process of OM as a function of time (Joffre et al., 1992; Sabetta et al., 2006). It should be noted that the decomposition of OM in soils differs from that of OM in controlled environments, such as composting plants, where the water content and ventilation are regulated.

The use of hyperspectral spectroscopy directly in the compost plant has been suggested as a means of detecting and controlling the presence of contaminants (Bonifazi et al., 2008; Dall'Ara et al., 2012) rather than their stability. Attempts to address the abovementioned need have been suggested in a small number of studies in which the composting processes of grape marc and cattle manure (Ben-Dor et al., 1997), municipal sewage sludge and trimmings (Albrecht et al., 2008), and plant materials, such as leaf litter and grasses (Gillon et al., 1999b, 1993; Joffre et al., 1992), were studied in conjunction with hyperspectral spectroscopy.

Insights from these studies, among others (Ben-Dor et al., 1997; Curran, 1989; Paz-Kagan et al., 2014), indicated that the reflected light in the visible (VIS, 400–700 nm), near infrared (NIR, 700–1100 nm), and shortwave infrared (SWIR, 1100–2500 nm) spectral regions is energetic enough to excite overtones and combinations of molecular vibrations to higher energy levels. Therefore, the biosolids' characteristics and number of functional groups, such as the chemical bonds —CH, —OH, and —NH, give a unique spectral signature that can be used to identify changes occurring during the composting process. McMorrow et al. (2004) found correlations between cellulose, lignin, and a water content decrease during composting and the SWIR transmission. These variables alone cannot be used as indicators for compost maturity. Other researchers showed that compost total C, organic C, C:N, sulfur (S), potassium (P), and pH were correlated to the NIR spectra in dry material (Albrecht et al., 2008; Malley et al., 2005).

Commonly, hyperspectral studies employ either air-dried (Ben-Dor et al., 1997; Gillon et al., 1999b) or oven-dried samples (Albrecht et al., 2008; Gillon et al., 1993; Joffre et al., 1992) since the water signal can mask other physicochemical characteristics of the target material (Waiser et al., 2007). However, air drying and/or pre-heating of the OM sample, such as soil, may change its surface properties (e.g., water content, color) and, consequently,

the reflectance spectrum (Mzuku et al., 2015). Specifically, while the overall content may not be affected, the chemical nature at the surface may vary as a result of the reorientation and/or configuration of OM functional groups (Arye et al., 2007; Ellerbrock et al., 2005). This, in turn, may increase the relative share of more hydrophobic functional groups at the surface (Aderibigbe et al., 1997), which may be expressed in the reflectance.

The above studies indicate a gap of knowledge regarding the applicability of the hyperspectral method for evaluating selected maturation parameters such as dissolved organic carbon (DOC), nitrate-nitrogen ( $\text{NO}_3^-$ -N), and ammonium-nitrogen ( $\text{NH}_4^+$ -N) content and its use on samples at their natural water content. The assessment of compost maturity by hyperspectral reflectance requires establishing a dataset in which measured chemical parameters are correlated with reflectance analysis. From this analysis, we may make conclusions regarding the applicability of this method.

The main objective of this study was to examine the applicability of hyperspectral analyses for characterizing the time-dependent process of biosolids composting. In this context, the reflectance spectra were correlated with quantitative and qualitative chemical properties, obtained from the solid and liquid phases of the examined biosolids, in both their moist and oven-dried states.

## 2. Materials and methods

### 2.1. Sampling

The biosolids used in this experiment were obtained from a commercial municipal sewage sludge composting plant (Compost Or Ltd, Israel). The first sampling took place immediately after the sewage sludge was mixed with trimmings. Over the next two months, the biosolids were sampled once a week in triplicates from the same pile. After two months, the pile from which the biosolids were sampled was sieved through 8 mm sieves, as part of the commercial composting procedure. Thereafter, the pile was transferred to the experimental station located at the Sede Boqer Campus of Ben-Gurion University and was sampled every 1–2 weeks in the following month and once a month for the following two months. Samples from a total of 15 sampling dates were taken for hyperspectral and chemical analyses. In each sampling event, the sampled biosolids were divided into two portions: one portion was stored at 4 °C until used and the other was placed in the oven (105 °C for 48 h). The gravimetric water content on the sampling date was calculated from the difference between the wet and dry weights.

### 2.2. Chemical analysis

The chemical analysis was carried out in triplicates for both the liquid and solid phases of the compost. For the former, the wet or dry compost samples were extracted by mixing them with double distilled water at a ratio of 1:10 (w/w). Thereafter, the samples were filtered through a 0.45- $\mu\text{m}$  membrane and measured for the DOC, total nitrogen ( $\text{TN} = \text{NO}_3^-$ -N +  $\text{NH}_4^+$ -N + dissolved organic nitrogen),  $\text{NH}_4^+$ -N and  $\text{NO}_3^-$ -N concentrations. DOC and TN were analyzed with a total organic carbon analyzer (Shimadzu Corporation, Japan) equipped with a total nitrogen measuring unit. The  $\text{NH}_4^+$ -N and  $\text{NO}_3^-$ -N concentrations were measured with an ultraviolet–visible spectrophotometer (Evolution 220, Thermo Scientific). The  $\text{NH}_4^+$ -N concentration was determined using the Nessler method (Nichols and Willits, 1934; Yuen and Pollard, 1954), and the  $\text{NO}_3^-$ -N concentration was determined using the second-derivative ultraviolet spectrophotometric method. Each sample

was scanned from 200 to 250 nm, and the maximum value was calculated from the second derivative of the spectra, from which the  $\text{NO}_3^-$ -N concentration was obtained (Eaton et al., 2005). Using this method, one can efficiently eliminate the organic matter background, commonly prevalent in compost extracts. The results were reported on a dry weight basis corrected to the initial water content. Total C and N were determined for the oven-dried samples after grinding using the CHNS elemental analyzer (organic elemental analyzer, FlashEA 1112, THERMO Fisher Scientific Inc., USA).

### 2.3. Hyperspectral analysis

Biosolid samples were brought to room temperature and thereafter spectrally measured for reflected data by an Analytical Spectral Devices (ASD) FieldSpec Pro FR spectrometer with a spectral range of 350–2500 nm and a 25° field of view (FOV). The spectral sampling resolution was 1.4 nm for 350–1000 nm and 2 for 1000–2500 nm. The spectrometer was programmed to average 40 spectra per sample. A standard white reference panel (Spectralon Labsphere Inc.) was used as a white reference (Hatchell, 1999). The distance of the bare fiber from the target was 8 cm; therefore, the FOV was a circle with a radius of 1.77 cm. To reduce directional effects, the samples were illuminated from two directions, and each sample was spectrally measured four times; after each measurement, it was rotated by 90°. The four repetitions for each sample were averaged and considered as a spectral sample. The spectral data was clipped to the range of 400–2400 nm to avoid noisy spectral data at the two edges due to the relatively low quantum efficiency of the detectors. Finally, the spectral resolution was reduced to 10 nm, resulting in 200 spectral bands from 405 to 2395 nm.

The area under the spectra between 1100 nm and 1460 nm and the area between 1940 nm and 2400 nm were calculated to the zero line for the dry and wet samples. The ratio between the two area values was calculated.

### 2.4. Modeling approach

Spectral samples were obtained on 15 different dates. The chemical and the corresponding spectral measurements resulted in a dataset containing 146 spectra and chemical data. Each of the spectra was related to several chemical properties. This main dataset was divided into two portions: one for dry biosolids (88 samples) and the other for wet ones (58 samples). Each of these datasets was divided into calibration (about 75%) and prediction sets (about 25%). The calibration set was used to calibrate the model, and the prediction set was used for spectrally predicting the values of the measured chemical parameters. The data were randomly sorted and only then divided for calibration and prediction.

In order to predict each of the chemical properties by spectral means, the partial least squares-regression (PLS-R) analysis was applied in a Matlab 7.6 (MathWorks, Natick, MA, USA) environment using the PLS-toolbox (Eigenvector, Wenatchee, WA, USA). The PLS-R is a practical predictive tool for spectral reflective data (Hansen and Schjoerring, 2003; Nguyen and Lee, 2006). Its prediction was chosen since it can analyze continuous spectra and deal efficiently with the multi-collinearity present among the reflectance values of hyperspectral data (Atzberger et al., 2010; Wold et al., 2001). To assess the quality of the PLS-R model prediction, the root mean square error (RMSE) of prediction (RMSEP) was calculated as presented by Wise et al. (2006), by one equation:

$$\text{RMSE} = \sqrt{\frac{\sum_{i=1}^n (\hat{y}_i - y_i)^2}{n}} \quad (1)$$

where  $\hat{y}_i$  is the predicted value of the variable when the sample number  $i$  is not included in the model formation, and  $n$  is the number of prediction samples (the PLS-R calibration models comprised 67 dry samples and 43 wet samples; the prediction PLS-R models included 21 dry samples and 15 wet samples).  $y_i$  is the measured value of the variable. To evaluate the relative importance of each wavelength in each of the PLS-R models, the variable importance in projection (VIP), after Wold et al. (1993), was computed. The VIP is defined as the summary of the importance for each predictor (wavelength) in all projections (principal components) of the PLS-R model (Chong and Jun, 2005; Cohen et al., 2010; Herrmann et al., 2011). The VIP is computed as each predictor's importance with the explained sum of squares by the PLS-R dimension, summed for all dimensions related to the total explained sum of squares by the PLS-R model and for the total number of predictors. Therefore, it is an indicator of each predictor's (in this case, the spectral data's wavelengths) relative power and influence in the PLS-R model. The VIP averaged value per sample is one. This value is considered to be the putative VIP threshold. It was also used in the current study, and the VIP values above it were considered as highly influencing the PLS model (Olah et al., 2004). Wavelengths peaking with VIP values that were above the threshold were checked in the literature for specific chemical bonds.

## 3. Results and discussion

Attempts to use hyperspectral analysis as a method to assess compost maturity and quality were performed in several studies (Albrecht et al., 2008; Ben-Dor et al., 1997; Gillon et al., 1999a, 1993; Joffre et al., 1992). However, none of these studies were carried out on samples at their original water content but rather on either air-dried or oven-dried samples. In addition, the above studies indicate a gap in knowledge regarding the applicability of the hyperspectral method for evaluating selected maturation parameters such as: DOC,  $\text{NO}_3^-$ -N, and  $\text{NH}_4^+$ -N contents. In this study, a hyperspectral analysis was used in order to predict the chemical nature of biosolids' composted OM as a function of composting time. Given the impact of water content on the sample reflectance, both wet and dry samples were examined. The reason for this is twofold: (i) to examine hyperspectral changes in the biosolids during their decomposition with and without the water absorption interferences; and (ii) to be able to assess the compost stability and maturity at the composting plant, under natural conditions.

Fig. 1A and B present the reflectance spectra of the dry and wet samples, respectively, from the 15 sampling events. The results demonstrate the differences between these two groups. In both cases, the samples' albedo gradually increased from each sampling date to the following one, reaching its highest value after 78 days, followed by a slight decrease. The difference between the reflectance of the litter decomposition and of the sewage sludge decomposition is that the former starts green and turns black and the latter starts dark and the change is at a smaller intensity. This is the reason why as opposed to the current results, Ben-Dor et al. (1997) found that the albedo of litter decreases during its decomposition. Some changes in the reflectance spectra that can be visualized are marked in Fig. 1A and B, and the chemical functional groups commonly related to them (Ben-Dor et al., 1997; Curran, 1989; Elvidge, 1990; Paz-Kagan et al., 2014) are summarized in Table 1. In the wet and dry samples, at around 1200 nm, an absorbance feature that is an indicator band was observed. The absorbance was more intense on the first sampling dates, and it diminished with time. The absorbance in this wavelength is commonly related to water, cellulose, starch, lignin and oil (Table 1). Although lignin and cellulose are considered to be more resistant to microbial degradation, their content is reduced during biosolids

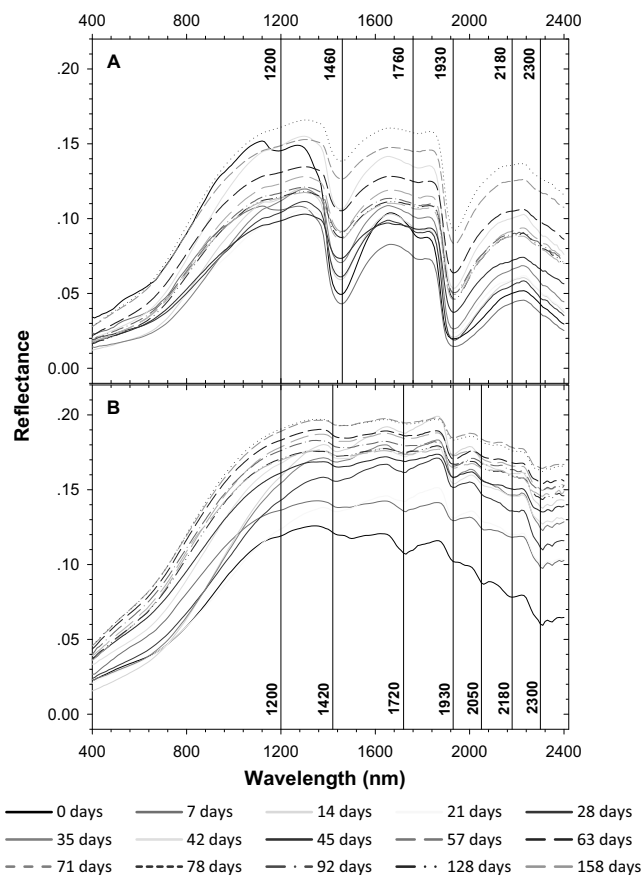


**Fig. 1.** Hyperspectral reflectance of the biosolids during their decomposition. (A) Wet samples (natural water content). (B) Dry samples (105°). Vertical lines indicate diagnostic absorbance features as described in Table 1.

decomposition thanks to the microorganisms that make use of the carbohydrates originating from the degradation of cellulose as a source of energy (Jouraiphy et al., 2005). The wet samples showed two distinct absorbance features that are indicator bands around 1460–1490, and 1930 nm (Fig. 1A) and are assigned to OH in water. The high absorbance of water masked other features close to them. Therefore, features observed in the dry samples, such as 1420 and 2050 nm (see also Table 1), that provided information about the chemical composition of the biosolids were not seen in the wet ones. At the same time, there was a shift of the absorbance at 1720 nm in the dry samples compared with 1760 nm in the wet samples. These features were attributed to the aliphatic C–H stretch. The absorption around 2180 and 2300 nm was again

attributed to chemical compounds that broke up during the OM decomposition (Table 1), and therefore, their absorbance intensity decreased with the biosolids decomposition. In addition, also in that area, a slight influence of the water content could be seen; hence, the intensity of the absorption between 2000 and 2400 nm was much lower in the wet samples in comparison with the dry samples. Waiser et al. (2007) reported that air-drying increases the accuracy of the prediction model as drying reduces the absorbance intensity of bands related to water signals, and therefore, it does not mask other physicochemical properties. This finding corroborates our current results.

The PLS-R approach was applied to create a predication tool for the biosolids' chemical composition. The starting point was the establishment of a correlation between the spectral data and a given measured parameter. Specifically, the hyperspectral data were correlated with the variables obtained from the chemical analysis. As mentioned, the chemical and spectral analyses were carried out initially with the wet samples (i.e., the naturally moister ones) and then with the same samples after drying them at 105 °C for 48 h in order to obtain dry samples with no traces of water. In the following, the results are presented for the liquid extraction that was performed for both wet and dry samples and for the solid elemental analysis that was carried out only on the dry ones. Selected results from the prediction of the PLS-R model are presented in Fig. 2, and a summary of all of the correlations is presented in Table 2. The coefficient of determination,  $R^2$ , and the RMSE express the prediction accuracy of each variable and the likelihood of the measured data falling within the predicted outcome. The VIP values based on the PLS-R models are presented in Fig. 3.

The general pattern obtained for all of the maturity variables (excluding the  $\text{NO}_3^-$ -N) as a function of composting time exhibited an exponential-like decay (Figs. 4 and 5). Similar patterns were also obtained for the ratio between the areas under the spectra between wavelengths 1100–1460 nm and 1940–2400 nm (Fig. 6). The bands in the range of 1100–1460 nm are usually assigned, aside from the O–H bends in water molecules, to the C–H and N–H stretches in aliphatic groups. The bands in the range of 1940–2400 nm are also assigned to the C=C, C=O, N=H and O=H stretches in aromatic rings, carboxyl, and ketonic carbonyl groups (Ben-Dor et al., 1997; Curran, 1989). These findings are in agreement with the decomposition of OM in which the aromatic compounds are more resistant to microbial breakdown. For further analysis, the data obtained from the PLS-R analysis are presented next to the measured data in each of the figures.

The C/N ratio increased to about 15 over the first 45 days, and from day 63 onward, it was around 11 (Fig. 5C and F). The final C/N ratio was  $11.07 \pm 1.04$ , which indicates a stable level of mature compost. Although the C/N was measured in the dry samples, the

**Table 1**  
Diagnostic wavelengths assigned to the major absorbance features shown in Fig. 1.

Wavelength (nm)	Chemical process	Associate elements
1200	O–H bend	Water <sup>β</sup> , cellulose <sup>αβ</sup> , starch <sup>αβ</sup> , lignin <sup>β</sup> , oil <sup>α</sup>
1420	C–H stretch	Lignin <sup>β</sup>
1460, 1490	O–H stretch	Water <sup>α</sup> , Cellulose <sup>αβ</sup> , sugar <sup>β</sup>
1720	Aliphatic C–H stretch	Cellulose <sup>α</sup> , lignin <sup>α</sup> , starch <sup>α</sup> , pectin <sup>α</sup> , wax <sup>α</sup> , humic acid <sup>α</sup> , nitrogen <sup>δ</sup>
1760	Aliphatic C–H stretch, O–H $\text{NO}_3$	Cellulose <sup>αβ</sup> , lignin <sup>α</sup> , starch <sup>αβ</sup> , sugar <sup>β</sup> , pectin <sup>α</sup> , wax <sup>α</sup> , humic acid <sup>α</sup>
1930	O–H stretch, –COOH, C=O of ketonic carbonyl, $\text{CONH}_2$ , $\text{NO}_3$	Water <sup>β</sup> , lignin <sup>αβ</sup> , protein <sup>β</sup> , nitrogen <sup>β</sup> , starch <sup>αβ</sup> , glucan <sup>α</sup> , cellulose <sup>αβ</sup> , pectin <sup>α</sup> , wax <sup>α</sup> , humic acid <sup>α</sup>
2050	N=H bend, N–H stretch, aromatic C=C, COO–Hydrogen bond, C=O	Protein <sup>β</sup> , nitrogen <sup>β</sup> , cellulose <sup>αγ</sup> , glucan <sup>α</sup> , pectin <sup>α</sup>
2180	Aromatic C=C, Amid II, N–H bend, C–H stretch, C–O stretch, C=O stretch, C–N stretch,	Starch <sup>α</sup> , lignin <sup>αγ</sup> , wax <sup>α</sup> , tannins <sup>α</sup> , Protein <sup>αβ</sup> , nitrogen <sup>β</sup> , $\text{NH}_4^+$ , $\text{NO}_3^-$ , Potassium <sup>δ</sup>
2300	C–H stretch, O–H stretch, $\text{CH}_2$ bend	Cellulose <sup>αβγ</sup> , sugar <sup>γ</sup> , starch <sup>αβ</sup> , $\text{CH}_3$ , Potassium <sup>δ</sup>

The assignments and chemicals are based on <sup>α</sup>Ben-Dor et al. (1997); <sup>β</sup>Curran (1989); <sup>γ</sup>Elvidge (1990) and <sup>δ</sup>Paz-Kagan et al. (2014).

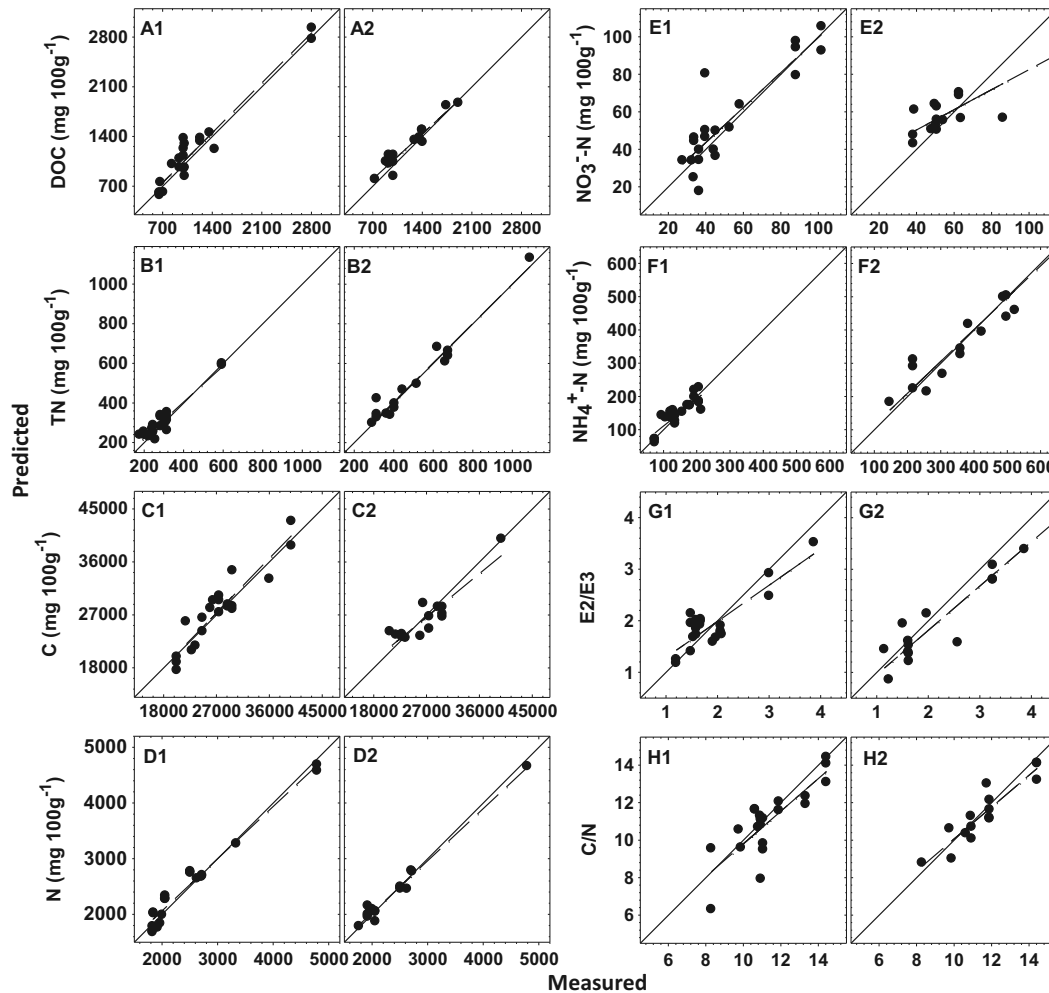


**Fig. 2.** Prediction of the model using the partial least squares-regression algorithm. (A1–H1) Dry samples (105 °C). (A2–F2) Wet samples (natural water content). (A1 and A2) Dissolved organic carbon (DOC) concentration; (B1 and B2) total dissolved nitrogen (TN) concentration; (C1 and C2) carbon (C) concentration; (D1 and D2) nitrogen (N) concentration. (E1 and E2)  $\text{NO}_3^-$ -N concentration; (F1 and F2):  $\text{NH}_4^+$ -N concentration; (G1 and G2) E2 to E3 ratio; (H1 and H2) C to N ratio. Solid line: prediction line 1:1, without intersects. Dashed line: trend line of the points, the real prediction line. The prediction line parameters are presented in Table 2.

**Table 2**

PLS-R prediction model results of the “Compost Or” decomposition process, 158 days, 15 sampling days. All  $R^2$  values are significant with  $P$  values < 0.001.

	Calibration LVs		Calibration				Prediction							
	Dry	Wet	Dry		Wet		Dry				Wet			
			$R^2$	RMSEC*	$R^2$	RMSEC*	$R^2$	$a$	$b$	RMSEP*	$R^2$	$a$	$b$	RMSEP*
DOC	12	8	0.96	93.8	0.85	129.9	0.94	1.00	46.4	154.9	0.92	0.91	156.2	104.3
TN	20	14	0.97	15.9	0.97	28.8	0.92	0.91	40.6	32.7	0.96	0.99	7.0	42.1
$\text{NO}_3^-$ -N	20	4	0.96	3.6	0.52	15.4	0.79	0.93	6.2	11.9	0.63	0.54	28.9	12.2
$\text{NH}_4^+$ -N	10	16	0.54	25.5	0.97	27.5	0.75	0.82	29.1	23.1	0.93	0.96	17.9	46.5
E2/E3	12	19	0.86	0.26	0.99	0.14	0.75	0.70	0.6	0.32	0.94	0.86	0.1	0.44
C	8	16	0.89	1747.8	0.95	1046.1	0.86	1.03	-456.7	2267.0	0.83	0.82	4538.8	1942.9
N	11	18	0.95	172.1	0.99	53.4	0.96	0.94	185.4	163.7	0.98	0.94	155.8	106.5
C/N	13	16	0.67	0.90	0.92	0.46	0.68	0.87	1.1	1.13	0.84	0.85	1.5	0.70

$R^2$ : coefficient of determination; (a) and (b): slope and intercept, respectively, of the regression line between the measured and predicted values of compost maturity parameters. LVs: latent variables; RMSEC: root mean square error of calibration; RMSEP: root mean square error of prediction; DOC: dissolved organic carbon; TN: total nitrogen;  $\text{N}-\text{NO}_3^-$ : nitrate nitrogen;  $\text{N}-\text{NH}_4^+$ : ammonium nitrogen; E2/E3: absorbance at 254/365 nm; C: carbon; N: nitrogen; C/N: carbon to nitrogen ratio. \*RMSEC and RMSEP units are  $\text{mg } 100 \text{ g}^{-1}$  for all except E2/E3 and C/N, which are dimensionless.

PLS-R model prediction was stronger (higher  $R^2$ ) for the wet samples than for the dry ones. Another indicator of compost maturity and stability is the DOC concentration. Fig. 4A and F exhibit the DOC concentration as a function of composting time for the wet and dry samples. According to the DOC values established by

Bernal et al. (1998) and Hue and Liu (1995) as the index for stable compost (values lower than  $1000 \text{ mg}/100 \text{ g}$ ), the biosolids in the recent study reached stability after about 75 days. After 158 days, the DOC concentration was about  $658 \text{ mg}/100 \text{ g}$  and  $517 \text{ mg}/100 \text{ g}$  for the dry and wet samples, respectively.

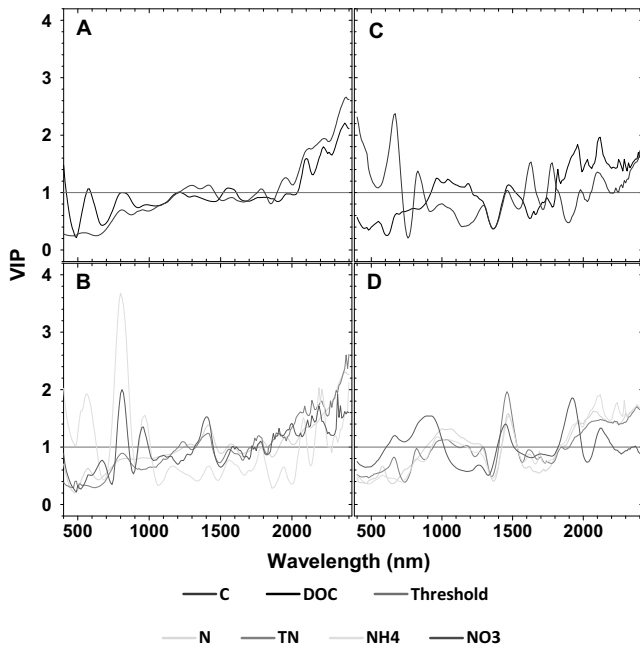


**Fig. 3.** Variable importance in projection (VIP) values based on the PLS-R model for the carbon (C), dissolved organic carbon (DOC), nitrogen (N), total nitrogen (TN), ammonium nitrate ( $\text{NH}_4\text{-N}$ ) and nitrate-nitrogen ( $\text{NO}_3\text{-N}$ ). (A and B): dry samples; (C and D): wet samples. The threshold to consider VIP values is 1.

Using the PLS-R model for the prediction of DOC concentration gave good results with  $R^2$  values of 0.92 and 0.94 for the wet and dry samples, respectively (Table 2, Fig. 2A and E). The RMSE of prediction was smaller for the wet samples than for the dry samples. Overall, the reestablishment of the predicted results in the time scale displayed small differences between the predicted and the measured results for most of the measured points, especially at the end of the biosolids decomposition – at the time of compost maturation (Fig. 4A). Although there were some outliers, the decomposition trend was predicted by the model.

The correlation described above is related to the quantity of the DOC, rather than to its chemical nature. The chemical nature of dissolved OM, in particular its molecular weight, can be evaluated in a qualitative manner from the bulk spectroscopic property, the E2/E3 ratio (absorbance at 254/365 nm; Chin et al., 1994). The E2/E3 ratio is inversely correlated with the molecular weight of the DOM (Peuravuori and Pihlaja, 1997). The higher portion of the compounds with smaller molecular size (higher ratio) at the first sampling event reduced rapidly with time (Fig. 4E and J) due to the decomposing process. As small volatile molecules are lost from the dissolved OM during oven drying (Schumacher, 2002), the  $R^2$  value of the prediction model for the wet samples was 0.94, while for the dry samples, the  $R^2$  value was 0.70.

The biosolids' chemical nature can also be related to the significant features in the reflectance spectra of a target material. The wavelength identified by VIP showing spectral regions (wide or narrow) that contributed to the model can be used for this purpose (Fig. 3). The wavelengths identified by VIP for the dry samples' DOC were all concentrated in the SWIR range (1000–2400 nm). The DOC contains various compounds, such as phenols, carboxylic acids, carbohydrates, groups with aromatic and aliphatic natures and other functional groups with low molecular weights (Haynes, 2005). Therefore, it is expected that a variety of wavelengths will be found to be important for this predictor projection. For example, the 2135 nm wavelength was assigned to the C=C of aromatic rings (Ben-Dor et al., 1997), and the 2235 nm was assigned to the C–H stretch in protein (Curran, 1989). Looking at the spectra,

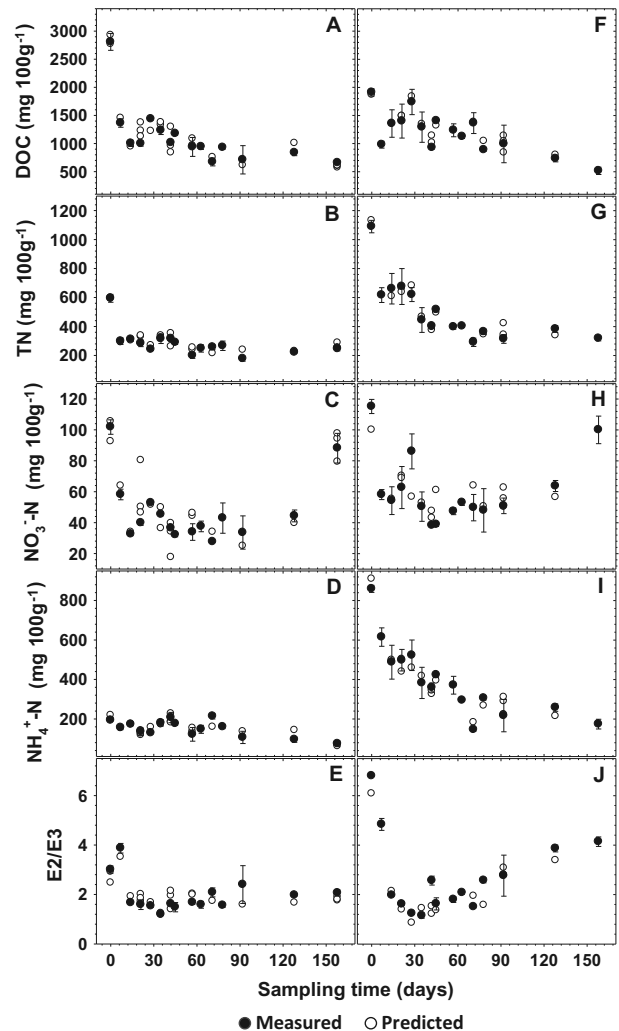


**Fig. 4.** Measured and predicted results from the PLS-R model. Left: oven-dried samples ( $105^\circ$ ). Right: wet samples (natural water content). (A and F) dissolved organic carbon (DOC) concentration; (B and G) total dissolved nitrogen (TN) concentration; (C and H) nitrate-nitrogen ( $\text{NO}_3\text{-N}$ ) concentration; (D and I) ammonium-nitrogen ( $\text{NH}_4\text{-N}$ ); (E and J) absorbance at 254/365 nm (E2/E3). Vertical bars indicate  $\pm 1$  standard deviation from the mean.

it can be seen that the magnitude of reflectance increased with the composting time, as expected, since the DOC component decomposed with time; hence, their absorbance decreased. Most of the wavelengths identified by VIP for the wet samples were also concentrated in the SWIR range (Fig. 3C), and most of them were in the same range of the dry samples. The high absorbance of the water in this region masks part of the wavelengths identified by the VIP in the dry samples. In addition, the PLS-R model found wavelengths identified by VIP for the wet samples in the red-edge and in the NIR region. These regions were most likely enhanced since the water masked part of the significant features in the SWIR range, and hence, the relative influence of the former increased.

The carbon content, measured at the solid phase of the biosolids, decreased by 51%, reaching a “plateau” about 75 days after the commencement of composting (Fig. 5A and D). Similar results were found by Zubillaga and Lavado (2003) for sewage sludge compost. The wavelength identified by the VIP for the PLS-R model of the C showed a similar trend to the DOC. Since the DOC is part of the total carbon, this behavior was expected. In addition, the PLS-R model for C identified more wavelengths, at 1200 and 1565 nm,

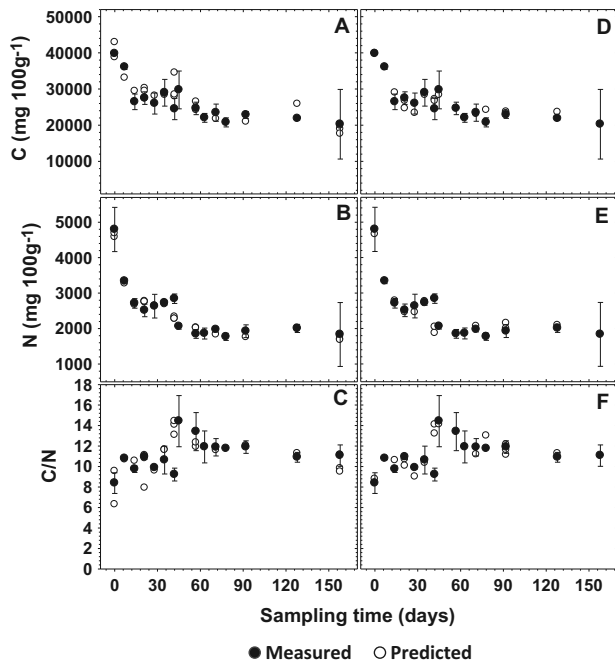


**Fig. 5.** Measured and predicted results from the PLS-R model as a function of time. Left: oven-dried samples ( $105^{\circ}$ ). Right: wet samples (natural water content). (A and D) carbon (C) concentration; (B and E) nitrogen (N) concentration; (C and F) carbon to nitrogen ratio (C/N). Vertical bars indicate  $\pm 1$  standard deviation from the mean.

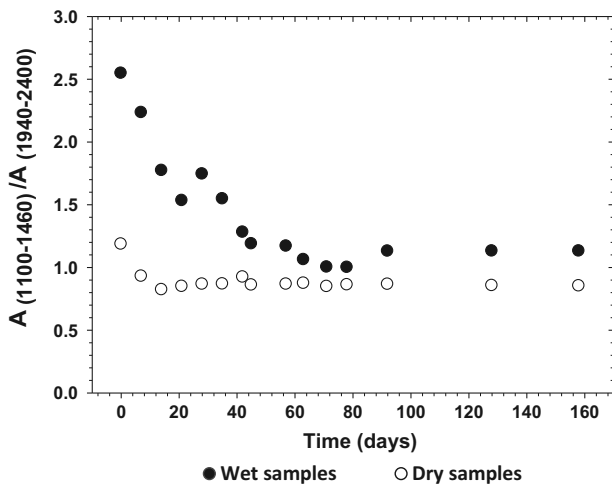


**Fig. 6.** The ratio between the areas under the spectra (A) between the wavelength range of 1100–1460 nm to the range of 1940–2400 nm as a function of time.

that can be assigned to the C–H overtone stretching (Golic et al., 2003) or to the O–H bends and stretches in starch and cellulose (Ben-Dor et al., 1997; Curran, 1989), most likely of insoluble molecules. The measured C and N concentrations used for the PLS-R model were the same for the wet and dry samples. Therefore, in this case, the accuracy can be tested for the model of each dataset directly from the RMSE. Table 2 shows no significant difference in the accuracy of the prediction model for the wet and dry samples of the C and N concentrations, implying that this method can be used with the wet samples, *in situ*, to evaluate compost maturity and stability.

During decomposition, the nitrogen undergoes a first stage of rapid decomposition of small molecular-sized compounds containing nitrogen, and thereafter, the more recalcitrant compounds

decompose much slower (Chen et al., 1997). The TN in the current study showed the same trend (Fig. 4B and G). However, the TN concentration in the dry samples was much lower since the TN in biosolids comprises mainly  $\text{NH}_4^+\text{-N}$  that volatilizes at  $105^{\circ}\text{C}$ . The ability to predict TN concentration in the biosolids was high for both the wet and dry samples and slightly stronger for the wet samples ( $R^2 = 0.92$  for the dry samples vs.  $R^2 = 0.96$  for the wet ones). On the other hand, the prediction accuracy for the dry samples was better (RMSEP = 32.7 for the dry samples vs. RMSEP = 42.1 for the wet samples). Most of the wavelengths identified by VIP for the TN in the dry samples were concentrated in the range of 1750–2400 nm (Fig. 3B). This area can be assigned to the N–H and N=H bands in proteins (Curran, 1989). Paz-Kagan et al. (2014) found that these wavelengths, together with 1255 and 1425 nm, can be assigned to  $\text{NO}_3^-$ . In the wet samples, the wavelengths could be still identified by VIP around 2100–2400 nm (Fig. 3D). However, in these samples, no wavelengths were identified around 1750–2000 nm, most likely due to the masking of the water absorbance in this area. On the other hand, the model of the wet samples did recognize the wavelengths around 1000–1100 nm that can be assigned to the N–H bands in proteins.

The  $\text{NH}_4^+\text{-N}$  concentration is a very important component in the N content in biosolids originating from sewage sludge (Smith et al., 1998). It followed the same trend as the TN, as can be seen in Fig. 4I. This was the case for the wet samples. As mentioned, for the dry samples, a significant portion of the  $\text{NH}_4^+\text{-N}$  was lost at  $105^{\circ}\text{C}$  (Fig. 4D and I). Therefore, the dry samples were not suitable for measuring the actual  $\text{NH}_4^+\text{-N}$  concentration. The PLS-R model was strong and accurate for the wet samples. For the dry samples, although the model was less strong and accurate, as expected (Table 2), it was still able to predict the low  $\text{NH}_4^+\text{-N}$  concentrations. The main bands that were found to be sensitive for  $\text{NH}_4^+$  content identification, using hyperspectral analysis (Paz-Kagan et al., 2014), were identified by the model for the dry samples (e.g., 575, 815 and 2225 nm, Fig. 3B). These bands were not identified by the model for the wet samples (Fig. 3D). However, other bands that are assigned to the N–H stretch (Curran, 1989) were identified as VIPs for the model (e.g., 1985, 2135, and 2305 nm).

The results of the measured and predicted nitrate for the dry and wet samples are presented in Fig. 4C and H. In the first stage of composting, there was leaching of a small compound, and therefore, a decrease in the nitrate content could be seen in the biosolids. At the next stage, mesophilic microorganisms converted organic N to ammonium and nitrate-N. Increasing levels of nitrate-N can be used as an indicator of maturing compost (García et al., 1991). The prediction model was stronger for the dry samples ( $R^2 = 0.79$ ) than for the wet ones ( $R^2 = 0.63$ ). It can be seen that for the dry samples, the model resulted in many narrow peaks of VIP values from 1600 to 2400 nm (Fig. 3B). Amongst them are wavelengths around 2180 nm that are directly related to  $\text{NO}_3^-\text{-N}$  (Table 1). However, for the wet samples, only five wide VIP peaks were identified (Fig. 3D). This shows the influence of water on the ability to identify narrow VIP peaks, related to  $\text{NO}_3^-\text{-N}$  in the SWIR region. Predicting  $\text{NO}_3^-\text{-N}$  using the PLS-R model was more successful for the dry than for the wet samples.

#### 4. Conclusions

This study was designed in order to examine the applicability of hyperspectral analysis to characterize the time-dependent process of biosolids composting. In order to achieve this goal, quantitative and qualitative chemical properties of wet and dry biosolid samples were correlated with reflectance spectra.

The results showed that the hyperspectral spectroscopy of biosolids can be used as a method to evaluate compost maturity and

stability. The spectra indicate the decrease in aliphatic compounds, in comparison to aromatic compounds, during the biosolids decomposition. The PLS-R model was able to predict with high accuracy the DOC, TN, C, and N contents in the wet and dry samples and the  $\text{NH}_4\text{-N}$  content and E2/E3 and C/N ratios for the wet samples.

In summary, the use of hyperspectral data analysis as a means to identify biosolids' chemical composition during composting was found to be suitable for both wet and oven-dried samples, excluding the correlation with the  $\text{NH}_4\text{-N}$  concentration, for which the wet samples yielded better results. The approach suggested in this study provides us with a simple and efficient (in terms of time and labor) method of identifying the compost maturity and stability stage in a biosolids composting site.

## Acknowledgements

This research project was supported by the Jacob Blaustein Institutes for Desert Research (BIDR). The authors wish to gratefully acknowledge the contributions of Compost Or Ltd. for helping us obtain samples.

## References

- Aderibigbe, A.O., Johnson, C.O.L.E., Makkar, H.P.S., Becker, K., Foidl, N., 1997. Chemical composition and effect of heat on organic matter- and nitrogen-degradability and some antinutritional components of Jatropa meal. *Anim. Feed Sci. Technol.* 67, 223–243. [http://dx.doi.org/10.1016/S0377-8401\(96\)01136-4](http://dx.doi.org/10.1016/S0377-8401(96)01136-4).
- Albrecht, R., Joffre, R., Gros, R., Le Petit, J., Terrom, G., Périssol, C., 2008. Efficiency of near-infrared reflectance spectroscopy to assess and predict the stage of transformation of organic matter in the composting process. *Bioresour. Technol.* 99, 448–455. <http://dx.doi.org/10.1016/j.biortech.2006.12.019>.
- Anne, N.J.P., Abd-Elrahman, A.H., Lewis, D.B., Hewitt, N.A., 2014. Modeling soil parameters using hyperspectral image reflectance in subtropical coastal wetlands. *Int. J. Appl. Earth Obs. Geoinf.* 33, 47–56. <http://dx.doi.org/10.1016/j.jag.2014.04.007>.
- Arye, G., Nadav, I., Chen, Y., 2007. Short-term reestablishment of soil water repellency after wetting: effect on capillary pressure-saturation relationship. *Soil Sci. Soc. Am. J.* 71, 692. <http://dx.doi.org/10.2136/sssaj2006.0239>.
- Atzberger, C., Guérf, M., Baret, F., Werner, W., 2010. Comparative analysis of three chemometric techniques for the spectroradiometric assessment of canopy chlorophyll content in winter wheat. *Comput. Electron. Agric.* 73, 165–173. <http://dx.doi.org/10.1016/j.compag.2010.05.006>.
- Bartholomeus, H.M., Schaepman, M.E., Kooistra, L., Stevens, A., Hoogmoed, W.B., Spaargaren, O.S.P., 2008. Spectral reflectance based indices for soil organic carbon quantification. *Geoderma* 145, 28–36. <http://dx.doi.org/10.1016/j.geoderma.2008.01.010>.
- Ben-Dor, E., Inbar, Y., Chen, Y., 1997. The reflectance spectra of organic matter in the visible near-infrared and short wave infrared region (400–2500 nm) during a controlled decomposition process. *Remote Sens. Environ.* 15, 1–15.
- Bernal, M., Navarro, A., Sánchez-monederó, M., Roig, A., Cegarra, J., 1998. Influence of sewage sludge compost stability and maturity on carbon and nitrogen mineralization in soil. *Soil Biol.* 30, 305–313.
- Boggs, J.L., Tsegaye, T.D., Coleman, T.L., Reddy, K.C., Fahsi, A., 2003. Relationship between hyperspectral reflectance, soil nitrate-nitrogen, cotton leaf chlorophyll, and cotton yield: a step toward precision agriculture. *J. Sust. Agric.* 22, 5–16. [http://dx.doi.org/10.1300/J064v22n03\\_03](http://dx.doi.org/10.1300/J064v22n03_03).
- Bonifazi, G., Serranti, S., D'Aniello, L., 2008. Compost quality control by hyperspectral imaging. *Proc. SPIE* 7003, 700321–700321-9. <http://dx.doi.org/10.1117/12.781639>.
- Cambardella, C.A., Richard, T.L., Russell, a., 2003. Compost mineralization in soil as a function of composting process conditions. *Eur. J. Soil Biol.* 39, 117–127. [http://dx.doi.org/10.1016/S1164-5563\(03\)00027-X](http://dx.doi.org/10.1016/S1164-5563(03)00027-X).
- Chen, Y., Inbar, Y., Chefetz, B., Hadar, Y., 1997. Composting and recycling of organic wastes. In: Rosen, D., Tel-Or, E., Hadar, Y., Chen, Y. (Eds.), *Modern Agriculture and the Environment*. Kluwer Academic Publishers, Dordrecht, The Netherlands, pp. 341–362. [doi:10.1007/978-94-011-5418-5\\_28](http://dx.doi.org/10.1007/978-94-011-5418-5_28).
- Chin, Y., Aiken, G., O'Loughlin, E., 1994. Molecular weight, polydispersity, and spectroscopic properties of aquatic humic substances. *Environ. Sci.* 1853–1858.
- Chong, I.-G., Jun, C.-H., 2005. Performance of some variable selection methods when multicollinearity is present. *Chemom. Intell. Lab. Syst.* 78, 103–112. <http://dx.doi.org/10.1016/j.chemolab.2004.12.011>.
- Cohen, Y., Alchanatis, V., Zusman, Y., Dar, Z., Bonfil, D.J., Karnieli, A., Zilberman, A., Moulin, A., Ostrovsky, V., Levi, A., Brikman, R., Shenker, M., 2010. Leaf nitrogen estimation in potato based on spectral data and on simulated bands of the VENμS satellite. *Prec. Agric.* 11, 520–537. <http://dx.doi.org/10.1007/s11119-009-9147-8>.
- Curran, P.J., 1989. Remote sensing of foliar chemistry. *Remote Sens. Environ.* 30, 271–278. [http://dx.doi.org/10.1016/0034-4257\(89\)90069-2](http://dx.doi.org/10.1016/0034-4257(89)90069-2).
- Dall'Ara, A., Bonoli, A., Serranti, S., 2012. An innovative procedure to characterize properties from tailored composites. *Manage. J.* 11, 2012.
- Eaton, A.D., Clesceri, L.S., Rice, E.W., Greenberg, A.E., 2005. Second-derivative ultraviolet spectrophotometric method. In: Eaton, A.D., Clesceri, L.S., Rice, E.W., Greenberg, A.E. (Eds.), *Standard Methods for the Examination of Water and Wastewater*. American Public Health Association (APHA), American Water works Association (AWWA), Water Environment Federation (WEF), Washington, pp. 121–122.
- Ellerbrock, R.H., Gerke, H.H., Bachmann, J., Goebel, M.-O., 2005. Composition of organic matter fractions for explaining wettability of three forest soils. *Soil Sci. Soc. Am. J.* 69, 57. <http://dx.doi.org/10.2136/sssaj2005.0057>.
- Elvidge, C.D., 1990. Visible and near infrared reflectance characteristics of dry plant materials. *Int. J. Remote Sens.* 11, 1775–1795.
- García, C., Hernández, T., Costa, F., 1991. Study on water extract of sewage sludge composts. *Soil Sci. Plant Nutr.* 37, 399–408. <http://dx.doi.org/10.1080/00380768.1991.10415052>.
- Gillon, D., Houssard, C., Joffre, R., 1999a. Using near-infrared reflectance spectroscopy to predict carbon, nitrogen and phosphorus content in heterogeneous plant material. *Oecologia*, 173–182.
- Gillon, D., Joffre, R., Dardenne, P., 1993. Predicting the stage of decay of decomposing leaves by near infrared reflectance spectroscopy. *Can. J. For.*
- Gillon, D., Joffre, R., Ibrahim, A., 1999b. Can litter decomposability be predicted by near infrared reflectance spectroscopy? *Ecology* 80, 175–186.
- Golic, M., Walsh, K., Lawson, P., 2003. Short-wavelength near-infrared spectra of sucrose, glucose, and fructose with respect to sugar concentration and temperature. *Appl. Spectrosc.* 57, 139–145. <http://dx.doi.org/10.1366/000370203321535033>.
- Hansen, P.M., Schjoerring, J.K., 2003. Reflectance measurement of canopy biomass and nitrogen status in wheat crops using normalized difference vegetation indices and partial least squares regression. *Remote Sens. Environ.* 86, 542–553. [http://dx.doi.org/10.1016/S0034-4257\(03\)00131-7](http://dx.doi.org/10.1016/S0034-4257(03)00131-7).
- Hargreaves, J., Adl, M., Warman, P., 2008. A review of the use of composted municipal solid waste in agriculture. *Agric. Ecosyst. Environ.* 123, 1–14. <http://dx.doi.org/10.1016/j.agee.2007.07.004>.
- Hatchell, D., 1999. *Analytical Spectral Devices, Inc. (ASD) Technical Guide*.
- Haynes, R., 2005. Labile organic matter fractions as central components of the quality of agricultural soils: an overview. *Adv. Agron.* 85, 221–268.
- Herrmann, I., Pimstein, a., Karnieli, a., Cohen, Y., Alchanatis, V., Bonfil, D.J., 2011. LAI assessment of wheat and potato crops by VENμS and Sentinel-2 bands. *Remote Sens. Environ.* 115, 2141–2151. <http://dx.doi.org/10.1016/j.rse.2011.04.018>.
- Hue, N.V., Liu, J., 1995. Predicting Compost Stability. *Compost Sci. Util.* 3, 8–15. <http://dx.doi.org/10.1080/1065657X.1995.10701777>.
- Joffre, R., Gillon, D., Dardenne, P., Agneessens, R., Biston, R., 1992. The use of near-infrared reflectance spectroscopy in litter decomposition studies. *Ann. des Sci. For.* 49, 481–488. <http://dx.doi.org/10.1051/forest:19920504>.
- Jouraihy, A., Amir, S., El Gharous, M., Revel, J.-C., Hafidi, M., 2005. Chemical and spectroscopic analysis of organic matter transformation during composting of sewage sludge and green plant waste. *Int. Biodeterior. Biodegradation* 56, 101–108. <http://dx.doi.org/10.1016/j.ibiod.2005.06.002>.
- Li, D., Chen, X., Peng, Z., Chen, S., Chen, W., Han, L., Li, Y., 2012. Prediction of soil organic matter content in a litchi orchard of South China using spectral indices. *Soil Till. Res.* 123, 78–86. <http://dx.doi.org/10.1016/j.still.2012.03.013>.
- Liu, H., Zhang, Y., Zhang, B., 2009. Novel hyperspectral reflectance models for estimating black-soil organic matter in Northeast China. *Environ. Monit. Assess.* 154, 147–154. <http://dx.doi.org/10.1007/s10661-008-0385-4>.
- Malley, D.F., McClure, C., Martin, P.D., Buckley, K., McCaughey, W.P., 2005. Compositional analysis of cattle manure during composting using a field-portable near-infrared spectrometer. *Commun. Soil Sci. Plant Anal.* 36, 455–475. <http://dx.doi.org/10.1081/CSS-200043187>.
- McMorrow, J.M., Cutler, M.E.J., Evans, M.G., Al-Roichid, A., 2004. Hyperspectral indices for characterizing upland peat composition. *Int. J. Remote Sens.* 25, 313–325. <http://dx.doi.org/10.1080/0143116031000117065>.
- Moral, R., Paredes, C., Bustamante, M.A., Marhuenda-Egea, F., Bernal, M.P., 2009. Utilisation of manure composts by high-value crops: safety and environmental challenges. *Bioresour. Technol.* 100, 5454–5460. <http://dx.doi.org/10.1016/j.biortech.2008.12.007>.
- Mzuku, M., Khosla, R., Reich, R., 2015. Bare soil reflectance to characterize variability in soil properties. *Commun. Soil Sci. Plant Anal.* 46, 1668–1676. <http://dx.doi.org/10.1080/00103624.2015.1043463>.
- Nguyen, H.T., Lee, B.-W., 2006. Assessment of rice leaf growth and nitrogen status by hyperspectral canopy reflectance and partial least square regression. *Eur. J. Agron.* 24, 349–356. <http://dx.doi.org/10.1016/j.eja.2006.01.001>.
- Nichols, M., Willits, C., 1934. Reactions of Nessler's Solution. *J. Am. Chem. Soc.* 56, 769–774.
- O'Rourke, S.M., Holden, N.M., 2012. Determination of soil organic matter and carbon fractions in forest top soils using spectral data acquired from visible-near infrared hyperspectral images. *Soil Sci. Soc. Am. J.* 76, 586. <http://dx.doi.org/10.2136/sssaj2011.0053>.
- Olah, M., Bologna, C., Oprea, T.I., 2004. An automated PLS search for biologically relevant QSAR descriptors. *J. Comput. Aided Mol. Des.* 18, 437–449. <http://dx.doi.org/10.1007/s10822-004-4060-8>.
- Ozores-Hampton, M., Peach, D., 2002. Biosolids in vegetable production systems. *Horttechnology* 12.

- Paz-Kagan, T., Shachak, M., Zaady, E., Karnieli, A., 2014. A spectral soil quality index (SSQI) for characterizing soil function in areas of changed land use. *Geoderma* 230–231, 171–184. <http://dx.doi.org/10.1016/j.geoderma.2014.04.003>.
- Peuravuori, J., Pihlaja, K., 1997. Molecular size distribution and spectroscopic properties of aquatic humic substances. *Anal. Chim. Acta* 337, 133–149. [http://dx.doi.org/10.1016/S0003-2670\(96\)00412-6](http://dx.doi.org/10.1016/S0003-2670(96)00412-6).
- Rigby, H., Perez-Viana, F., Cass, J., Rogers, M., Smith, S.R., 2009. The influence of soil and biosolids type, and microbial immobilisation on nitrogen availability in biosolids-amended agricultural soils – implications for fertiliser recommendations. *Soil Use Manag.* 25, 395–408. <http://dx.doi.org/10.1111/j.1475-2743.2009.00240.x>.
- Sabetta, L., Zaccarelli, N., Mancinelli, G., Mandrone, S., Salvatori, R., Costantini, M.L., Zurlini, G., Rossi, L., 2006. Mapping litter decomposition by remote-detected indicators 49, 10.
- Schumacher, B., 2002. Methods for the determination of total organic carbon (TOC) in soils and sediments. *Ecol. Risk Assess.* Support Cent.
- Shah, Z., Jani, Y.M., Khan, F., 2014a. Evaluation of organic wastes for composting. *Commun. Soil Sci. Plant Anal.* 45, 309–320. <http://dx.doi.org/10.1080/00103624.2013.861909>.
- Singh, R.P., Agrawal, M., 2008. Potential benefits and risks of land application of sewage sludge. *Waste Manage.* 28, 347–358. <http://dx.doi.org/10.1016/j.wasman.2006.12.010>.
- Smith, S., Woods, V., Evans, T., 1998. Nitrate dynamics in biosolids-treated soils. I. Influence of biosolids type and soil type. *Bioresour. Technol.* 66, 139–149.
- Som, M.-P., Lemée, L., Amblès, a., 2009. Stability and maturity of a green waste and biowaste compost assessed on the basis of a molecular study using spectroscopy, thermal analysis, thermodesorption and thermochemolysis. *Bioresour. Technol.* 100, 4404–4416. <http://dx.doi.org/10.1016/j.biortech.2009.04.019>.
- Waiser, T.H., Morgan, C.L.S., Brown, D.J., Hallmark, C.T., 2007. In situ characterization of soil clay content with visible near-infrared diffuse reflectance spectroscopy. *Soil Sci. Soc. Am. J.* 71, 389. <http://dx.doi.org/10.2136/sssaj2006.0211>.
- Wise, B.M., Gallagher, N.B., Bro, R., Shaver, J.M., Windig, W., Koch, R.S., 2006. PLS\_Toolbox Version 4.0 for use with MATLAB TM. Eigenvector Research Inc, Wenatchee, WA, USA.
- Wold, S., Johansson, E., Cocchi, M., 1993. PLS- partial least squares projections to latent structures. In: Kubinyi, H. (Ed.), *3D QSAR in Drug Design: Theory, Methods, and Applications*. ESCOM, Leiden, pp. 523–550.
- Wold, S., Sjöström, M., Eriksson, L., 2001. PLS-regression: a basic tool of chemometrics. *Chemom. Intell. Lab. Syst.* 58, 109–130.
- Wu, L., Ma, L.Q., Martinez, G.a., 2000. Comparison of methods for evaluating stability and maturity of biosolids compost. *J. Environ. Qual.* 29, 424. <http://dx.doi.org/10.2134/jeq2000.00472425002900020008x>.
- Yuen, S., Pollard, A., 1954. Determination of nitrogen in agricultural materials by the nessler reagent. II.—Micro-determinations in Plant Tissue and in Soil Extracts. *Sci. Food Agric.* 5, 364–369.
- Zubillaga, M.S., Lavado, R.S., 2003. Stability indexes of sewage sludge compost obtained with different proportions of a bulking agent. *Commun. Soil Sci. Plant Anal.* 34, 581–591. <http://dx.doi.org/10.1081/CSS-120017841>.